

Intrinsic defect energies of lithium hydride and lithium deuteride crystals

Ravindra Pandey† and A M Stoneham

Theoretical Physics Division, AERE Harwell, Oxon OX11 0RA, UK

Received 4 March 1985

Abstract. A theoretical study has been made of the defect structure of lithium hydride and lithium deuteride. A potential model is obtained describing the statics and dynamics of these crystals. Intrinsic defect energies are calculated using the Harwell HADES program which is based on a generalised Mott–Littleton method. The results are in good agreement with the experimental data, and suggest that the vacancy and interstitial migration mechanisms of anions and cations are all comparable in their contribution to ionic conduction.

1. Introduction

The hydride and deuteride of lithium represent two of the simplest ionic crystals and, apart from their intrinsic scientific interest, are also representatives of the hydrides that may have important technological applications such as in fuel hydrogen storage. These crystals possess the rocksalt structure, with only four electrons in the primitive unit cell. In the ideal fully ionic state, both the cation and anion have the closed-shell configuration of the helium atom. In addition, these crystals exhibit a large isotope effect in both cation (^6Li and ^7Li) and anion (^1H , ^2H , ^3H) sublattices.

In a series of studies, Pretzel and his co-workers described the preparation and properties of lithium hydride (LiH) and lithium deuteride (LiD) single crystals (Pretzel *et al* (1962) and the earlier papers from the same group cited in this reference). They proposed models for some of the irradiation-induced point defects analogous to those in the alkali halide family using the optical absorption and electron paramagnetic resonance techniques. Anderson and Luty (1983) reported the luminescence emission produced by unspecified defects in these crystals, whereas Miki and Ikeya (1982) explained the results of a thermoluminescence study of irradiated crystals by proposing the formation of Frenkel pairs and the mobility of hydrogen interstitials at extremely low temperatures. From ionic conductivity curves, the Schottky pair formation energy and cation migration energy have been deduced (Ikeya 1977, Varotsos and Mourikis 1974). However, the Frenkel pair formation energies and anion migration energy are still unknown. Theoretical studies, on the other hand, have been limited to lattice dynamics calculations (Dyck and Jex 1981, Verble *et al* 1968). Thus, the results obtained from experimental and theoretical studies represent a far from satisfactory knowledge of the intrinsic defect structure of these crystals.

† Physics Department, University of Manitoba, Winnipeg (Manitoba), Canada R3T 2N2.

In an attempt to expand our physical understanding of the defect properties of these crystals, we have made a theoretic study which is based on lattice simulation techniques that have proved reliable for ionic and semi-ionic crystals. Our analysis intentionally concentrates on the parallel with alkali halides. Clearly, other classes of defect are possible, e.g. ones based on molecular ions such as Li_2^+ and H_2^+ , or centres based on atomic species H^0 or Li^0 ; H^0 , in particular, is known as a substitutional and interstitial defect in alkali halides. We find, nevertheless, that the bulk of the existing experimental data can be understood quantitatively within the framework of Schottky and Frenkel disorder.

2. Theoretical methods

In the present study, the intrinsic defect structure of the lattice has been simulated using the HADES code (Lidiard and Norgett 1972, Norgett 1974) which divides the lattice into two regions: an inner region I immediately surrounding the defect, where the lattice configuration is evaluated explicitly using pairwise potentials which represent the ionic interactions, and an outer region II which can be treated by the Mott–Littleton approximation using information on macroscopic response functions, namely the elastic and dielectric constants of the lattice. This code has been successfully applied to a wide variety of defect calculations in alkali and alkaline-earth halides, alkali, alkaline-earth, transition-metal and actinide oxides (Mackrodt (1982) and references therein), zinc selenide (Harding and Stoneham 1982) and calcium sulphide (Pandey and Harding 1984).

We take a fully ionic model based on Li^+ and H^-/D^- ions. Such a model is supported by the Hartree–Fock calculations by Dovesi *et al* (1984) and it is also consistent with much work on hydrogen defect centres in alkali halides (see, e.g., Stoneham (1975), ch 20). The value we use, $Z = 1$, within a shell model contrasts with the value $Z = 0.875$ used by Wilson and Johnson (1970), who combined a rigid-ion model with non-radial forces. The fits to perfect-crystal data are comparable in success; however, the use of $Z = 1$ is more transparent physically and avoids many problems associated with the definition of the energies of charged defects.

The ionic interactions can be represented as the sum of long-range Coulomb interactions and short-range non-coulombic interactions caused by the overlap of the electron clouds of the two ions. We use a pair potential description of the short-range potential which is a simple analytical expression of the Born–Mayer form:

$$V_{ij}(x) = A_{ij} \exp(-x/\rho_{ij}). \quad (1)$$

This may be supplemented by short-range attractive terms, that is, terms in x^{-6} and x^{-8} , often (but without good reason) attributed to ‘dispersion forces’; we shall include only the x^{-6} part. We use the shell model, originally proposed by Dick and Overhauser (1958) to simulate the ionic polarisation. In this model, the ionic polarisation is described by the displacement of a massless charged shell from a massive charged core, the two being connected by a harmonic spring. This allows dielectric properties of the crystal to be simulated accurately. The inter-ionic potential energy may therefore be expressed as a sum of pairwise terms of the form

$$\begin{aligned} \varphi_{ij}(\mathbf{r}, W_i, W_j) = & Z_i Z_j e^2 / |\mathbf{r}| + Y_i Y_j e^2 / |\mathbf{r} + \mathbf{W}_j - \mathbf{W}_i| + Y_i Z_j e^2 / |\mathbf{r} - \mathbf{W}_i| \\ & + Y_j Z_i e^2 / |\mathbf{r} + \mathbf{W}_j| + (e^2/2\nu)(K_i W_i^2 + K_j W_j^2) + V_{ij}(\mathbf{r}, W_i, W_j) \end{aligned}$$

where $\mathbf{r} \equiv (\mathbf{r}_j - \mathbf{r}_i)$ is the position of ion core j relative to ion core i , \mathbf{W}_i and \mathbf{W}_j the shell-core displacements, Y_i and Y_j the shell charges, K_i and K_j the spring constants, Z_i and Z_j the core charges of ions i and j , e the electronic charge, v the volume and V_{ij} the short-range part, assumed to act between the shells only.

The lattice potential energy contains the parameters that are to be determined. There are three short-range parts of the potential, V_{HH} , V_{LiLi} and V_{LiH} for LiH crystal and V_{DD} , V_{LiLi} and V_{LiD} for LiD crystal. These potentials have been obtained as described below.

(i) V_{HH} and V_{DD} (the anion-anion short-range interactions) are obtained by using the theoretical models developed by Wedepohl (1967) and Gordon and Kim (1972). These models are based on the density functional treatment of the uniform electron gas. Here, the electronic structure of the H^- ion in the Madelung potential field is calculated to obtain the ionic wavefunctions. Then this is pairwise superimposed, leading to inter-ionic pair interaction on the basis of the assumption that the charge densities of two isolated ions are unchanged when they are brought together, the resultant charge density being a simple superposition of the two. The computer program for this procedure is given by Harding and Harker (1982).

(ii) V_{LiLi} (the cation-cation short-range interaction) is taken to be independent of the crystal environment. Since this interaction is small at Li-Li separation, this assumption should not cause significant error. We have taken V_{LiLi} from the shell model of lithium fluoride (Catlow *et al* 1977) which has nearly the same lattice spacing as that of both LiH and LiD.

(iii) We use an empirical method to obtain V_{LiH} and V_{LiD} (the cation-anion short-range interactions). In this method, short-range parameters are determined in such a way that the model potential reproduces the observed macroscopic crystal data, namely the cohesive energy, lattice spacing, elastic constants and dielectric constants. This method has been successfully applied for a wide range of halides, oxides and sulphides. Note here that the short-range potential includes a part due to the difference between D and H zero-point motion. This dynamical component can, we find, be chosen to represent well the perfect-crystal properties of both LiH and LiD. We are, however, making the assumption that the same dynamical potential is transferable, i.e. it will

Table 1. Parameters of the short-range potential $V_{ij} = A_{ij} \exp(-r/\rho_{ij}) - C_{ij}r^{-6}$, together with values for the shell charge and spring constant.

Potential	A_{ij} (eV)	ρ_{ij} (Å)	C_{ij} (eV Å ⁶)
$V_{\text{HH}}/V_{\text{DD}}$	6611.11	0.1315	0.98
V_{LiLi}	1153.80	0.1364	0.0
V_{LiH}	188.57	0.3215	0.0
V_{LiD}	18.46	0.3197	0.0
		Shell charge, e	Spring constant (eV Å ⁻²)
LiH	Li ⁻	0.998	40.08
	H ⁻	-1.005	4.24
LiD	Li ⁺	0.998	40.99
	D ⁻	-1.005	4.03

describe short-range interactions near defects as well as in the perfect solid. R Ball, J H Harding and A M Stoneham (unpublished work) are developing a self-consistent phonons code to verify assumptions like this.

The resulting potentials are given in table 1. The values of A and ρ for Li-Li and Li-H(D) are similar to those of Wilson and Johnson (1970; in this comparison we consider their spherically averaged potentials). Our H-H (D-D) potential is repulsive, however, whereas theirs is attractive with shorter range.

It is interesting that the values of ρ for the LiH and LiD interactions are both about $\frac{1}{3}$ Å, i.e. in line with values for many ionic crystals. This is also consistent with values for other hydride-metal short-range interactions deduced from local mode frequencies of defects (by E Wade and A M Stoneham in unpublished work performed in 1979) and from the combination of hydride phonon data and local mode frequencies (Browne 1982).

3. Results and discussion

3.1. The perfect crystal

The calculated and the observed properties of LiH and LiD are listed in tables 2 and 3 respectively. It can be seen that they are reproduced quite well for all but C_{12} , which by virtue of the pairwise interaction of the ions is inevitably overestimated. The Cauchy violation is, in fact especially large in LiH and LiD and can only be partly accounted for even by long-range three-centre potentials (Wendel and Zeyher 1980) although the Dyck and Jex (1981) deformation dipole model is able to give a good fit with 13 adjustable parameters. Likewise, the Jaswal and Dilly (1977) 9-parameter fit gave reasonable lattice dynamics. However, these workers discuss only harmonic properties and do not provide a potential suitable for defect modelling. The Wilson and Johnson (1970) potential gives somewhat better values for C_{12} than ours, although only at the expense of less good values of the lattice parameter (their Model I) or cohesive energy (their Model II).

We have tested the reliability of our potential model by calculating the phonon dispersion curves in the principal symmetry directions using the lattice dynamics package

Table 2. Properties of lithium hydride.

	Calculated	Observed
(i) Lattice constant (Å)	2.0417	2.0417 ^a
(ii) Cohesive energy (eV)	-10.36	-9.44 ^a
(iii) Elastic constants (10 ¹² dyn cm ⁻²)		
C_{11}	7.98	7.41 ± 0.2 ^b
C_{12}	4.59	1.42 ± 0.03
C_{44}	4.57	4.84 ± 0.18
(iv) Dielectric constants		
ϵ_0	13.92	12.9 ± 0.5 ^c
ϵ_x	3.32	3.61 ± 0.5
(vi) Melting point (K)	—	961 ^c

^a Pretzel *et al* (1962).

^b James and Kheyrandish (1982).

^c Brodsky and Burstein (1967).

Table 3. Properties of lithium deuteride.

	Calculated	Observed
(i) Lattice constant (\AA)	2.0324	2.0324 ^a
(ii) Cohesive energy (eV)	-10.43	-9.63 ^a
(iii) Elastic constants (10^{12} dyn cm ⁻²)		
C_{11}	7.78	7.68 ± 0.2^b
C_{12}	4.67	1.51 ± 0.03
C_{44}	4.67	4.94 ± 0.18
(iv) Dielectric constants		
ϵ_0	14.78	14.0 ± 0.5^c
ϵ_∞	3.45	3.63 ± 0.5
(v) Melting point (K)	—	951 ^c

^a Pretzel *et al* (1962).

^b James and Kheyrandish (1982).

^c Brodsky and Burstein (1967).

developed by Sangster and Rowell (in 1983 (unpublished)) from the Harwell PHONONS program. The calculated dispersion curves are shown in figure 1 along with the observed spectra from an inelastic neutron scattering experiment for LiD crystal (experimental data are available for LiD only). We also have compared the frequency ratio $\omega(\text{LiH})/\omega(\text{LiD})$ with those from the lattice dynamics calculations of Verble *et al* (1968), based on a seven-parameter shell model fitted to neutron data on LiD in table 4. The overall agreement seems surprisingly good, keeping in mind the simplicity of our model. We may therefore conclude that our potentials, although simplified, provide a good approximate description of the harmonic statics and dynamics of LiH and LiD crystals.

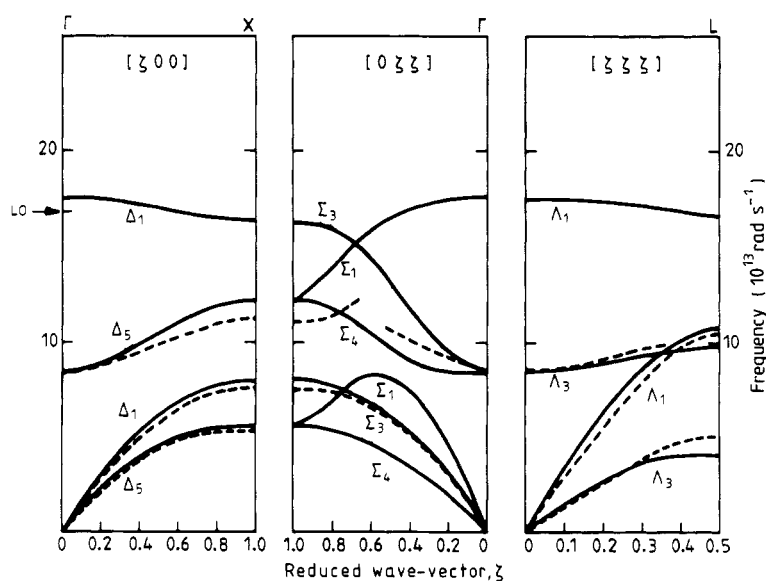

Figure 1. Phonon dispersion curves for LiD predicted with the present potentials (full curves) and compared with the experimental data of Verble *et al* (1968) (broken curves).

Table 4. Calculated frequency ratios $\omega(\text{LiH})/\omega(\text{LiD})$ for Γ -, X- and L-point phonons of LiH and LiD.

Phonon branch	Calculated frequency ratios					
	Present study			Verble <i>et al</i> (1968)		
	Γ	X	L	Γ	X	L
LO	1.35	1.38	1.43	1.33	1.39	1.40
TO	1.36	1.42	1.44	1.33	1.39	1.40
LA	—	1.04	0.99	—	0.99	0.97
TA	—	1.00	1.01	—	1.00	0.97

3.2. Defect energies

In table 5 we present our calculated defect formation energies in these crystals. The energies appear to be in good agreement with the experimental values. We define the formation energy of a vacancy as that required to remove a lattice ion to infinity, allowing the remaining lattice to relax to equilibrium. Likewise, the interstitial formation energy is that involved in bringing an ion from infinity to an interstitial site with corresponding relaxation of the surrounding lattice. The Schottky pair formation energy (E_S) is then the sum of the energies of formation of isolated cation and anion vacancies, reduced by the energy of the removed ions placed at the surface, which is given in terms of the cohesive energy. The Frenkel pair energy (E_F) is the energy of formation of an isolated vacancy and an isolated interstitial. The antisite defect is either a Li^+ ion at an H^- site or a D^- ion at a Li^+ site. Table 5 also contains the energies for the antisite defect pair, predicting that such defects are unlikely to be observed in these crystals in the form $(\text{H}_{\text{Li}}^- + \text{Li}_{\text{H}}^+)$. However, we have not looked at possibilities like H_{Li}^0 or $(\text{H}_2^-)_{\text{Li}}$, nor at molecular species like H_2^0 in cation–anion divacancies (note that H_{Li}^0 reacting with a host H^- ion produces H_2^- in a divacancy).

The Schottky pair formation energy of LiH is greater than that of LiD which is in line with the usual rule that the formation energy increases with the increase in crystal melting point. Our calculation clearly shows the isotope effect in these crystals, subject to our earlier remarks about transferability of potentials. The calculated formation energy of a Schottky pair is somewhat less than that of either Frenkel pair, thereby

Table 5. Intrinsic defect energies (eV).

	LiH		LiD	
	Calculated	Observed	Calculated	Observed
Schottky pair	2.42	2.30 ± 0.3^a 2.33 ± 0.01^b	2.29	2.40 ± 0.01^b
Frenkel pair				
anion	2.70	—	2.61	—
cation	2.72	—	2.65	—
Antisite pair (Li^+) _H + (H^-) _{Li}	7.81	—	7.98	—

^a Ikeya (1977).^b Varotsos and Mourikis (1974).

suggesting that vacancies, rather than interstitials, will be the most common defect species in both the crystals. However, interstitial defects prove to have a lower motion energy, and several mechanisms may contribute to ionic conduction.

We have calculated the activation energies for the migration of both anions and cations by vacancy and interstitial mechanisms. The activation energy is the energy of the saddle-point configuration relative to the isolated vacancy or interstitial. The saddle-point configuration consists of either a face-centred interstitial ion and two adjacent vacancies in the $\langle 110 \rangle$ direction for the vacancy mechanism, or a single face-centred ion for the interstitial mechanism. Note that these are classical (saddle-point) configurations rather than those for the small-polaron model used for H in metals (Flynn and Stoneham 1970). A corresponding calculation with the small-polaron model is possible, and is planned for later work; it will certainly be necessary if we are to interpret data on muon spin rotation. The calculated classical results are given in table 6 with the appropriate experimental results, and predict nearly the same activation energies for migration for both of the ions in these crystals.

Table 6. Activation energies for migration (eV).

	Vacancy mechanism		Interstitial mechanism	
	Calculated	Observed	Calculated	Observed
LiH				
Li ⁺	0.42	0.54 ± 0.02^a	0.17	—
H ⁻	0.40	—	0.19	—
LiD				
Li ⁺	0.33	0.52 ± 0.01^b	0.18	—
D ⁻	0.32	—	0.17	—

^a Ikeya (1977).

^b Varotsos and Mourikis (1974).

The experimental value of about 0.5 eV has been reported for the migration of a cation vacancy. Our calculated energies are lower than this value in both the crystals. However, the analysis of the conductivity curves has been made by assuming that the mobile species are cation vacancies which occur as extrinsic defects due to the presence of divalent cations in the lattice (Ikeya 1977, Varotsos and Mourikis 1974). The experimental value is therefore the activation energy in the presence of associated impurities in the lattice, whereas the calculated energy is for free cation–vacancy migration. Thus, a lower calculated activation energy would be expected (see, e.g., Mackrodt 1982) as obtained in the present case.

Furthermore, the above-mentioned analysis appears to require an activation energy for anion–vacancy migration that is twice that of the cation. However, contrary to this expectation, our calculation predicts nearly the same activation and Arrhenius energies for both the ions (table 7); indeed, this is inevitable when the dominant interactions are coulombic and nearest-neighbour pairwise forces, as used here for LiH and LiD. The assumption of immobility of anion vacancies in the reported experimental analyses is therefore questionable. Because of the near equality in the calculated Arrhenius energies, the ratio of cation and anion contributions to conductivity will be independent of the temperature. The situation is still more complex because we predict very similar Arrhenius energies for interstitials and vacancies. These various mechanisms could give

Table 7. The Arrhenius energy of migration (eV). (The Arrhenius energy is the slope of the ionic conductivity curve and, in an intrinsic region of a crystal, is half of the Schottky pair formation energy plus the vacancy migration energy for a vacancy mode of migration (Case I) or half of the Frenkel pair formation energy plus the interstitial migration energy for an interstitial mode of migration (Case II)).

	Observed	Calculated	
		Case I (vacancy)	Case II (interstitial)
LiH	1.70 ± 0.1^a	Li ⁻ 1.63	1.53
	1.720 ± 0.005^b	H ⁻ 1.61	1.54
LiD	1.695 ± 0.005^b	Li ⁻ 1.47	1.51
		D ⁻ 1.46	1.47

^a Ikeya (1977).

^b Varotsos and Mourikis (1974).

a nearly linear conductivity curve which could scarcely be resolved in the analysis of conductivity curves.

4. Conclusions

In summary, we have obtained an apparently reliable potential model for LiH and LiD crystals and have predicted that both the interstitial and vacancy modes of migration are important for ionic conduction in these crystals. The relative contributions from both anions and cations to the conductivity in the intrinsic region is found here to be almost independent of the temperature.

Acknowledgment

The authors are grateful to Dr J H Harding and Professor J Vail for useful discussions. One of us (RP) acknowledges financial support from AERE Harwell and NSERC Canada.

© 1985 UKAEA

References

- Anderson A and Luty F 1983 *Phys. Rev. B* **28** 3415
 Brodsky M H and Burstein E 1967 *J. Phys. Chem. Solids* **28** 1655
 Browne A M 1982 *PhD Thesis* University of Oxford
 Catlow C R A, Diller K M and Norgett M J 1977 *J. Phys. C: Solid State Phys.* **10** 1395
 Dick B G and Overhauser A W 1958 *Phys. Rev.* **112** 90
 Dovesi R, Ermondi C, Ferrero E, Pissani C and Roetti C 1984 *Phys. Rev. B* **29** 3591
 Duck W and Jex H 1981 *J. Phys. C: Solid State Phys.* **14** 4193
 Flynn C P and Stoneham A M 1970 *Phys. Rev. B* **1** 3966
 Gordon R G and Kim Y S 1972 *J. Chem. Phys.* **56** 3122
 Harding J H and Harker A H 1982 *AERE Report* R10425
 Harding J H and Stoneham A M 1982 *J. Phys. C: Solid State Phys.* **15** 4649

- Ikeya M 1977 *J. Phys. Soc. Japan* **42** 168
James B W and Kheyrandish H 1982 *J. Phys. C: Solid State Phys.* **15** 6321
Jaswal S S and Dilly V D 1977 *Phys. Rev. B* **15** 2366
Lidiard A B and Norgett M J 1972 *Computational Solid State Physics* ed. F Herman, N W Dalton and R G Kochler (New York: Plenum) p 385
Mackrodt W C 1982 *Computer Simulation of Solids* ed. C R A Catlow and W C Mackrodt (New York: Springer) p 175
Miki T and Ikeya M 1982 *J. Phys. Soc. Japan* **51** 2862
Norgett M J 1974 *AERE Report* R7650
Pandey R and Harding J H 1984 *Phil. Mag. B* **49** 135
Pretzel F E, Gritton G V, Rushing C C, Friauf R J, Lewis W B and Waldstein P 1962 *J. Phys. Chem. Solids* **23** 325
Stoneham A M 1975 *Theory of Defects in Solids* (Oxford: OUP)
Varotsos P A and Mourikis S 1974 *Phys. Rev. B* **10** 5220
Verble J L, Warren J L and Yarnell J L 1968 *Phys. Rev.* **168** 980
Wedepohl P T 1967 *Proc. Phys. Soc.* **92** 79
Wendel H and Zeyher R 1980 *Phys. Rev. B* **21** 5544
Wilson W D and Johnson R A 1970 *Phys. Rev. B* **1** 3510